

# Entropic contributions to the splicing process in Eukaryotes.

M. Osella, M. Caselle

*Dipartimento di Fisica Teorica and INFN, Università degli Studi di Torino, v. Pietro Giuria 1, 10125, Torino, Italy*

(Dated: February 14, 2019)

It has been recently argued that the depletion attraction may play an important role in different aspects of the cellular organization, ranging from the organization of transcriptional activity in transcription factories to the formation of the nuclear bodies. In this paper we suggest a new application of these ideas in the context of the splicing process, a crucial step of mRNA maturation in Eukaryotes. We shall show that entropy effects and the resulting depletion attraction may explain the relevance of the aspecific intron length variable in the choice of the splice-site recognition modality. On top of that, some qualitative features of the genome architecture of higher Eukaryotes can find an evolutionary realistic motivation in the light of our model.

Intron excision from pre-mRNAs is one of the most important steps in messenger RNA (mRNA) maturation. It is carried out by the spliceosome, which catalyses the intron removal and the assembly of exons into mature mRNA. The spliceosome assembly seems to proceed in a stepwise manner [1] that firstly requires the correct recognition of the intron/exon boundaries by snRNPs (small nuclear ribonucleoproteins) and splicing factors, and subsequently the splice-site pairing, which implies a looping of the intron. This assembly pathway and the molecular players are remarkably conserved through different species. Recent studies [2] have shown that splicing may follow two alternative pathways which are called *intron definition* and *exon definition* respectively. Intron definition (see Fig.1a) begins with the direct interaction of the U1 snRNP with the 5' splice site. The 3' splice site is then recognized by the U2 snRNP and associated auxiliary factors such as U2AF and SF1 [1, 2]. When the two complexes are constructed on the intron/exon boundaries they can be juxtaposed, closing an intron loop which is then spliced away in order to correctly glue the exons. The interaction of the splicing factors bound at the splice sites occurs in this case across the intron. The exon definition (see Fig.1b) requires instead that the initial interaction between the factors bound at the splice sites occurs across the exon: the U1 and U2 snRNP and associated splicing factors bind to the 3' and 5' ends of an exon and a complex is built across it (usually with the participation of SR proteins); then complexes on different exons join together so as to allow intron removal.

It has been recently shown [3] that the splice-site recognition modality is a function of the length of the intron that has to be removed. Short introns are spliced away preferentially through intron definition, while longer introns seem to require an exon definition process. In particular the analysis of [3] suggests the presence of a threshold in intron length (between 200 and 250 nt long) above which intron-defined splicing ceases almost completely. Lower Eukaryotes present typically short introns, below the threshold, so it is expected that intron removal proceeds through intron definition. Higher Eukaryotes instead have an intron length distribution presenting two pronounced peaks, with the threshold in between (see fig.2), so even if the vast majority of introns

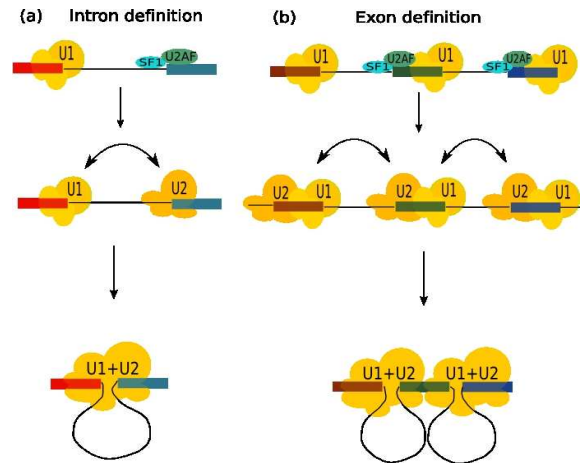


FIG. 1: Intron definition and exon definition: two ways of splice-site recognition.

are above the threshold (data in table I), the first peak represents intron suitable for intron definition. As it can be seen in fig.2, not only the shape of the distribution is quite conserved through different species, but also the position of the peaks.

The main goal of our paper is to propose a simple physical model which might explain this behaviour. Remarkably enough, despite its simplicity the model is able to produce quantitative predictions which are in rather good agreement with experimental observations.

Our starting point is the observation that the splicing complexes, which are immersed in the crowded nuclear environment, feel the so called “depletion attraction” [5]. This interaction is essentially an entropic effect due to the fact that when two large complexes (like the splicing ones) approach each other, they create an “excluded volume” between them. If the complexes are immersed in an environment crowded of macromolecules of smaller (but comparable) size, then this excluded volume effect induces an attractive interaction between the two complexes. Since the two complexes are joined by a freely fluctuating RNA chain this interaction becomes effectively long range, with a logarithmic like dependence on the chain length. We suggest that this depletion attrac-

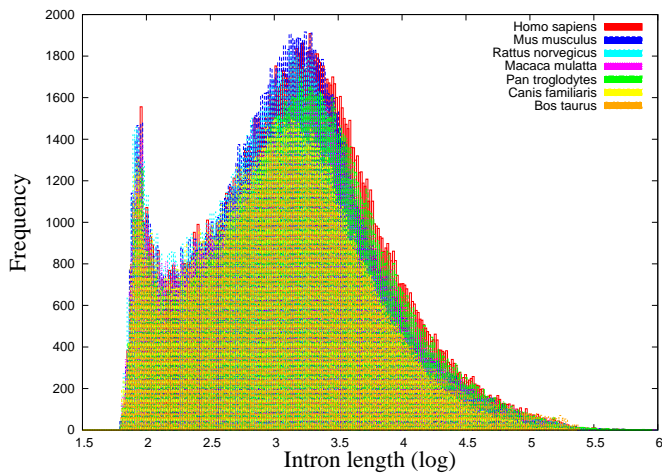


FIG. 2: Intron length distribution for different higher Eukaryotes. The distribution shows a two peaks structure which is remarkably universal. The intron length threshold mentioned in the text is located exactly between the two peaks. The right peak contains mostly introns which undergo exon-defined splicing, while the left one can be associated to intron-defined spliced introns. The coordinates of introns used were downloaded from the Ensembl database vers.47 [4].

tion is the driving force which allows the splicing complexes to meet and join one another, in order to start up the splicing process. As we shall see this assumption naturally leads to a smooth cross-over from an intron defined to an exon defined splicing pathway as the chain length increases.

Let us model, as a first approximation, the pre-mRNA as a Freely Jointed Chain (FJC), i.e a succession of infinitely penetrable segments, each of length  $l$ . The two complexes, composed by U1, U2 and splicing factors, that bind to exon/intron boundary in the intron definition process, will be modeled as spheres with a diameter  $D$  (the dimensions of the major components U1 and U2 are quite similar, both of the order of  $\sim 10$  nm, see [6] and [7] for details). The same geometrical approximation will be done for complexes constructed across exons in exon definition. They will be considered as spheres of diameter  $D'$ , with  $D' \sim 2D$  since they are composed by both the U1 and the U2 subcomplexes plus the exon in between, usually with SR proteins bound to it [2].

The simple FJC model allows the analytical calculation of the radial probability distribution of the end-to-end distance [8]:

$$W(r)dr = \left(\frac{\beta}{\sqrt{\pi}}\right)^3 4\pi r^2 \exp(-\beta^2 r^2) dr \quad (1)$$

where  $\beta = \left(\frac{3}{2nl^2}\right)^{\frac{1}{2}}$ ,  $n$  is the number of independent segments in the FJC and  $l$  is the length of a segment (in our case the Kuhn length of mRNA). Following [9], in order to include the depletion attraction contribution, we weighed the radial probability distribution of the end-

to-end distance (we assume that the ends of the intron can be considered as the center of the beads) with a Boltzmann factor, which takes into account the depletion attraction potential and which is non-zero in the range  $D \leq r \leq D + d$ . This potential is easy to evaluate in this “hard sphere” approximation (see for instance [5]) and takes a particularly simple expression in the  $d \ll D$  limit:

$$W(r) \exp \left\{ \frac{3}{2} c \frac{D}{d} \left( \frac{D + d - r}{d} \right)^2 \right\} dr \quad (2)$$

where  $c$  denotes the volumetric concentration of the small molecules and  $d$  their typical size. With the typical values of these quantities for the nuclear environment:  $c \sim 0.2$  and  $d \sim 5$  nm one finds for the problem at hand a potential energy of the order of one hydrogen bond, which is exactly in the range of energies needed to join together the two ends of an intron of length of about 10 Kuhn length (equivalent to 50 nucleotides).

The appealing feature of this model is that it introduces in a natural way a relation between the intron length and the dimensions of spliceosome subcomplexes attached to its ends, if we constrain the system to keep a fixed looping probability. This relation turns out to be roughly of logarithmic type.

This can be seen by looking at fig.3 where we plotted the looping probability for different intron lengths as a function of the diameter of the spheres attached to its ends. If we increase the intron length of an order of magnitude the beads’ diameter must be enlarged by a (roughly constant) multiplicative factor in order to obtain the same looping probability.

This observation may be used to explain the switch from intron to exon definition as the intron length increases. When the intron length becomes too large the dimensions of merely U1 and U2 subcomplexes is not enough to ensure a reasonable looping probability. This does not mean that such a process is forbidden but simply that it would require much longer times. For large enough introns it becomes more probable that the two complexes instead join across the exon. The complexes constructed across exons can actually result large enough to maintain a suitable looping probability, even in the case of long introns.

However, looking at fig.3 we see that while the model works nicely from a qualitative point of view it predicts intron lengths which are slightly smaller than those actually observed. In fact, in order to make the model more realistic and to be able to obtain also a quantitative agreement with the data, we must take into account two other ingredients. The first one is that pre-mRNAs can be bound to various regulatory proteins which have the effect of increasing their Kuhn length. Unfortunately no direct estimate of the Kuhn length in this conditions exists, thus to obtain the the curves reported in fig.3 we were compelled to use the Kuhn length of pure ssRNAs.

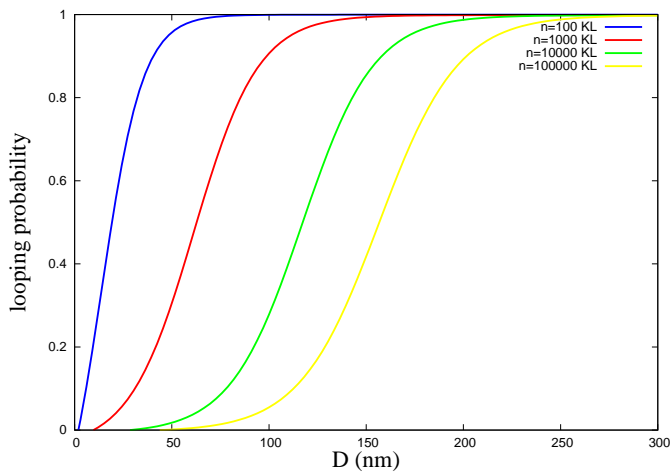


FIG. 3: We show the looping probability for different intron lengths as a function of the diameter of the spheres attached to the ends. Following [10] [11] the Kuhn length of the chain was fixed to 5 nt (about 3nm). However it is well known that many regulatory proteins can be bound to the pre-mRNAs and that the latter may fold into rather complex secondary structures. Both these factors have the effect of increasing the stiffness of the pre-mRNA thus increasing its Kuhn length. Unfortunately so far there are no experimental estimates of the Kuhn length in these conditions, so the value derived for ssRNA should be better considered as a lower bound. The diameter of the small crowding molecules is assumed as 5 nm (see [9] and references therein). The intron is considered as looped if the surfaces of the two spheres lie within a sufficiently short distance - chosen as 5 nm, in line with [9]-.

Hence the intron length reported in the figure should be better considered as lower bounds.

The second one is that the splicing (sub)complexes are rather far from the hard sphere approximation. If the irregular shape of the molecules permit a snugly fit or if parts of the two subcomplexes can intermingle, the free energy gain will be larger. Again this suggests that our results should be better considered as lower bounds. In this case however we can slightly improve our model and obtain also a reliable upper bound for our looping probability. The maximal relaxation of the hard hypothesis can be achieved considering that the two spheres can fuse with volume conservation (*soft hypothesis*). While we can't actually write the analytical expression of the potential in this "soft beads" case, it's undemanding to calculate the free energy gain obtained by the complete fusion of the two spheres. It's directly related to the portion of volume that becomes available to the crowding molecules:

$$\Delta F_{gain} = cK_B T \left( \frac{2(D+d)^3 - (2^{1/3}D+d)^3}{d^3} \right) \quad (3)$$

Following again [9] we may at this point assume that the functional dependence from  $r$  is the same of the hard-hypothesis scenario and write the weighed radial proba-

bility distribution, introduced in equation 2, as :

$$W(r) \exp \left\{ \left( \frac{2(D+d)^3 - (2^{1/3}D+d)^3}{d^3} \right) \left( \frac{D+d-r}{d} \right)^2 \right\} dr$$

From this expression it is straightforward to obtain the probability distribution of the end-to-end distance and obtain curves analogous to those reported in fig.3. The upper bounds for the looping probability are compared with those obtained in the hard-sphere case in fig.4, where we report the minimum diameter of the beads attached to the ends of the introns needed to have a looping probability of 99%. In fig.4 we also plot two vertical lines corresponding to the intron lengths of the left and right peak of the distribution in Fig.2 as typical values for the introns devoted to intron definition and exon definition respectively. Remarkably enough in both cases the actual dimensions of the splicing complexes (the black dots along the vertical lines in the figure) lie exactly in between the two bounds. Moreover looking at the curves it is easy to see that moving from the first to the second peak the subcomplexes size must increase roughly of the amount actually observed in the transition from intron definition to exon definition in order to keep the same looping probability.

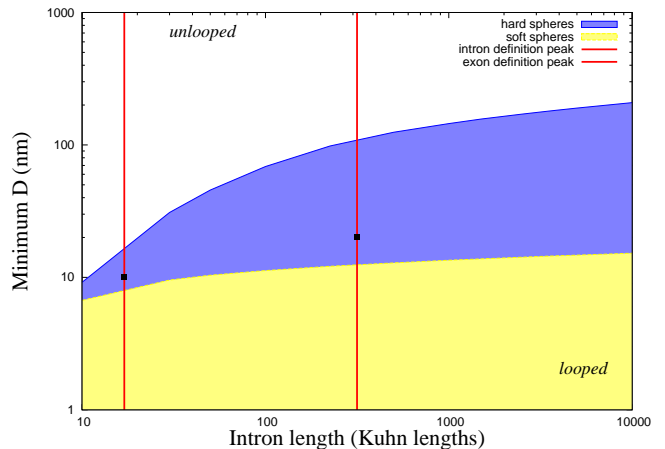


FIG. 4: Minimum diameter of beads attached to the ends of an intron needed to obtain a looping probability of 99%. The two curves correspond to the looping probability obtained in the hard and soft hypothesis respectively. The two vertical red lines correspond to the two peaks in the intron length distribution of *H. sapiens* (but are quite conserved through different higher Eukaryotes as can be seen in fig.2). Black squares represent the estimated diameter of spliceosome (sub)complexes for the two corresponding ways of splice site recognition. While for the intron-definition case estimates for the dimensions of the involved snRNP can be found in literature ([6], [7]), less information is known for the typical size of the complex constructed across exons in exon definition. In the figure we made the (rather conservative) assumption that the diameter of this complex is twice that of the subcomplexes involved in intron-defined splicing.

Species	Median	Mean of the gaussian fit	Percentage of exon-def introns
Homo sapiens	8	7.7	84
Canis familiaris	8	7.2	78
Pan troglodytes	8	7.8	83
Danio rerio	8	6.7	66
Macaca mulatta	8	6.5	79
Mus musculus	7	6.8	84
Rattus norvegicus	7	6.6	78
Gallus gallus	8	6.7	83
Bos taurus	8	6.8	81

TABLE I: For each species we report: the median (chosen instead of the mean because of the skewness of the distribution) of the overall distribution of the number of exons per gene (first column); the mean of the gaussian fit made over the same distribution, discarding the intronless genes (second column); the percentage of introns which undergo exon-defined splicing according to [3] (third column).

Obviously many other types of specific and elaborate regulation of the splicing dynamic are present in the cell, but the ATP-free depletion attraction could explain the widespread importance of the aspecific intron length variable.

So far we completely neglected the cooperative effects that could arise from the presence of more than two beads on the mRNA string. As discussed in [9], the pairing of more than two beads moves the energetic balance towards the free energy gain. For example, clustering three beads implies three excluded volumes that overlap, but only two loops that have to be closed; four beads give a sixfold free energy gain at the cost of closing only three loops, and so forth. However self avoidance cannot be neglected in this case, as crowding progressively makes the looping more energetically expensive. As observed in [9] (and reference therein) in three dimensions the entanglement constraints become important when more than eight beads cluster together. Above this threshold the free energy gain/loss ratio starts to decrease, setting the optimal number of beads around eight. In the framework of exon-defined splicing, each bead corresponds to a com-

plex constructed across an exon. Remarkably enough the median value of the number of exons per gene is strongly conserved in higher Eukaryotes (which make an extensive use of exon-defined splicing) and almost coincides with the optimal number of beads in the depletion attraction model (see tab.I and fig.5).

Many more refined and energetically costing mechanism of splicing are surely present in the cell, and many genes present a huge number of exons (up to about 490 in human), but the fact that the typical value is maintained in different organism around, or just below, eight, as predicted by the model, seems to suggest an evolutionary imprinting due to the depletion attraction role in exon juxtaposition.

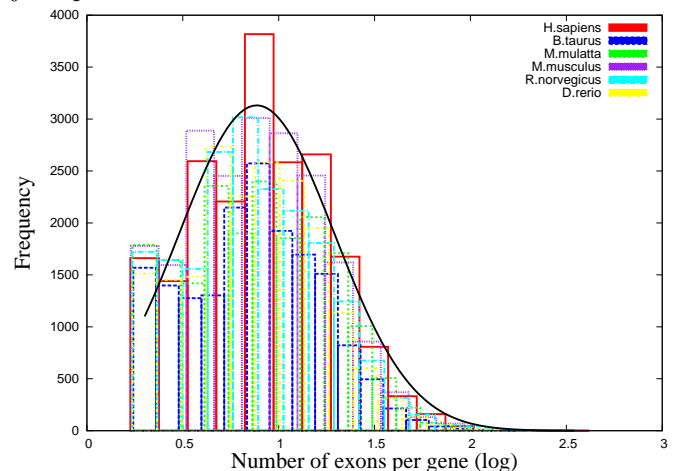


FIG. 5: Distribution of the exon number per gene for different higher Eukaryotes (data from [4]). Histograms of frequencies are constructed with a logarithmic binning, discarding the intronless genes. The continuous line is the result of a tentative gaussian fit to the H.sapiens distribution.

**Acknowledgements.** We thank U. Pozzoli and M.Cereda for very useful discussion and I. Molineris and G. Sales for technical support. This work was partially supported by the Fund for Investments of Basic Research (FIRB) from the Italian Ministry of the University and Scientific Research, No. RBNE03B8KK-006.

[1] M.J.Schellenberg et al., Trends Bioch.Sci. **33**, 243,(2008).  
[2] K.J.Hertel, J.Biol.Chem. **283**, 1211-1215,(2008).  
[3] K.L.Fox-Walsh et al., PNAS **102**,16176-16181,(2005).  
[4] P.Flicek et al., Nucl Acids Res **36**:,D707-D714,(2008).  
[5] S.Asakura and F.Oosawa, J.Chem.Phys. **22**,1255,(1954).  
[6] J.Sperling et al., Structure **16**,1605-1615,(2008).  
[7] B.Kastner et al., PNAS **87**,1710-1714,(1990).

[8] Cantor and Schimmel, "Biophysical Chemistry PartIII", W.H. Freeman and Company,(1980).  
[9] D.Marenduzzo et al., Biophys.J. **90**, 3712-3721,(2006).  
D.Marenduzzo et al., J.Cell Biol. **175**, 681-686,(2006).  
[10] K.Rippe, Trends Bioch.Sci.**26**,733-740,(2001).  
[11] J.Liphardt et al., Science **292**,733,(2001).